Compartmental and Spatial models in Biology

Sander Broos (11895616) & Nick van Santen (11857846)

I. Introduction

Biological processes often have a spatial component to their functionality. Oxygen needs to be transported from the lungs to the blood, embryos need to know the orientation to grow, fluids diffuse through a body. This makes it very useful to implement the spatial component in many biological models. This report will look into two methods to do this: multicompartmental ODEs and a grid based model.

The multicompartmental is created to study the dynamics of calcium concentrations within a cell. This is performed on a cell with three compartments: the endoplasmic reticulum (ER), the mitochondria, and calcium binding proteins in the cytosol. These compartments are linked with each other through calcium fluxes. With these fluxes ODEs are composed to study the concentrations of calcium in all three compartments. This is performed by looking at the time evolution of the system, plotting 2D and 3D phase plots and comparing peak values in the calcium concentrations through a lorentz map.

Furthermore, the Schnakenberg model is implemented, which is a reaction-diffusion model. In addition to molecules only reacting with each other, they also diffuse through space in this model. This added spatial component can give rise to so-called Turing patterns, which will be investigated in this report. This is done by discretising a 1D and a 2D environment into points separated by a constant interval, and approximating the behaviour of the model in discrete time steps.

II. Theory

THE multicompartmental model of the calcium concentrations in a cell will be derived in this section. This is achieved by looking into the ingoing and outgoing fluxes of the three compartments and combining them into a set of ODEs. Furthermore the Schnakenberg model is explained by its differential equations and the molecular reactions that define it.

A. Complex calcium oscillations

A cell model is created to study the dynamics of the calcium concentration in the cell. The model, initially created by Mahrl et al. [1], consists of three systems that control the concentration of calcium: the endoplasmic reticulum (ER), the mitochondria, and calcium binding proteins in the cytosol.

The calcium binding proteins in the cytosol undergo a reversible reaction with calcium.

$$\mathrm{Ca} + \mathrm{Pr} \rightleftharpoons \mathrm{CaPr}$$

Therefore the proteins control the available calcium in the cytosol. The mass action law gives the rate at which the reversible reaction occurs. Thus the production rate ν_+ of $CaPr$ is given by

$$\nu_+ = k_+[\mathrm{Ca_{cyt}}][\mathrm{Pr}] \tag{1}$$

, while the decay rate ν_- of $CaPr$ is given by

$$\nu_- = k_-[\mathrm{CaPr}] \tag{2}$$

The ER has three a total of three fluxes which control [Ca]. The first flux J_{pump} is a pump in the ER which pumps calcium from the cytosol into the ER. In the ER the calcium induces the release of Ca^{2+} back into the cytosol through the ER channels with flux J_{ch}. Some of the Ca^{2+} ions leak from the ER back into the cytosol with flux J_{leak}. The three fluxes are given by

$$J_{pump} = k_{pump}\mathrm{Ca_{cyt}} \tag{3}$$

$$J_{ch} = k_{ch}\frac{{\mathrm{Ca_{cyt}}}^2}{K_1^2 + {\mathrm{Ca_{cyt}}}^2}\left(\mathrm{Ca_{ER}} - \mathrm{Ca_{cyt}}\right) \tag{4}$$

$$J_{leak} = k_{leak}\left(\mathrm{Ca_{ER}} - \mathrm{Ca_{cyt}}\right) \tag{5}$$

, where k_{pump}, k_{ch}, k_{leak}, and K_1 are constant parameters, which control the magnitude of the flux.

A genetic mutation might occur in the ER, which could reduce the rate at which Ca^{2+} ions are transported through the ER channel, and thus reduce k_{ch}. The reduction in the effectiveness of the channel would result in a higher buildup of Ca in the ER. A complete failure of the channel would stop any Ca^{2+} ions from traveling through the channel, which means that the J_{ch} flux would be 0.

The mitochondria have one flux coming in J_{in} and one flux going out J_{out}. The mitochondria take in Ca^{2+} through its uniporters and leak small amounts of Ca^{2+}. These fluxes are given by

$$J_{in} = k_{in}\frac{{\mathrm{Ca_{cyt}}}^8}{K_2^8 + {\mathrm{Ca_{cyt}}}^8} \tag{6}$$

$$J_{out} = \left(k_{out}\frac{{\mathrm{Ca_{cyt}}}^2}{K_3^2 + {\mathrm{Ca_{cyt}}}^2} + k_m\right)\mathrm{Ca_m} \tag{7}$$

, where k_{in}, K_2, k_{out}, K_3, and k_m are constant parameters, which control the magnitude of the flux.

The calcium concentration is computed in all of the components. The cytosol has an inflow of J_{ch}, J_{leak}, J_{out}, and ν_-, while it has an outflow of J_{pump}, J_{in}, and ν_+. The ER has an inflow of J_{pump} and an outflow of J_{ch} and J_{leak}. The mitochondria have an inflow of J_{in} and an outflow of J_{out}. Three differential equations capture these

$$\begin{aligned}\frac{d[\mathrm{Ca_{cyt}}]}{dt} &= J_{ch} + J_{leak} - J_{pump} + J_{out} - J_{in} \\ &\quad + \nu_- - \nu_+ \\ &= J_{ch} + J_{leak} - J_{pump} + J_{out} - J_{in} \\ &\quad + k_-[\mathrm{CaPr}] - k_+[\mathrm{Ca_{cyt}}][\mathrm{Pr}]\end{aligned} \tag{8}$$

$$\frac{d[\mathrm{Ca_{ER}}]}{dt} = \frac{\beta_{ER}}{\rho_{ER}}\left(J_{pump} - J_{ch} - J_{leak}\right) \tag{9}$$

$$\frac{d[\mathrm{Ca_m}]}{dt} = \frac{\beta_m}{\rho_m}\left(J_{in} - J_{out}\right) \tag{10}$$

, where β_{ER} and β_m is the fraction of calcium of the total calcium concentrations for both the ER and mitochondria, and ρ_{ER} and ρ_m is the volume ratio between the ER and cytosol and mitochondria and cytosol, respectively.

The number of variables in these differential equations can be reduced by observing that the total concentration of calcium atoms $\mathrm{Ca_{tot}}$ and proteins $\mathrm{Pr_{tot}}$ remain constant in the system and are given by

$$\begin{aligned}Ca_{tot} &= [\mathrm{Ca_{cyt}}] + \frac{\rho_{ER}}{\beta_{ER}}[\mathrm{Ca_{ER}}] + \frac{\rho_m}{\beta_m}[\mathrm{Ca_m}] \\ &\quad + [\mathrm{CaPr}]\end{aligned} \tag{11}$$

$$Pr_{tot} = [\mathrm{Pr}] + [\mathrm{CaPr}] \tag{12}$$

These can be rewritten to obtain values for $[\mathrm{CaPr}]$ and $[\mathrm{Pr}]$

$$[\mathrm{CaPr}] = \mathrm{Ca_{tot}} - [\mathrm{Ca_{cyt}}] - \frac{\rho_{ER}}{\beta_{ER}}[\mathrm{Ca_{ER}}] \tag{13}$$

$$- \frac{\rho_m}{\beta_m}[\mathrm{Ca_m}] \tag{14}$$

$$\begin{aligned}[\mathrm{Pr}] &= \mathrm{Pr_{tot}} - [\mathrm{CaPr}] \\ &= \mathrm{Pr_{tot}} - \mathrm{Ca_{tot}} + [\mathrm{Ca_{cyt}}] \\ &\quad + \frac{\rho_{ER}}{\beta_{ER}}[\mathrm{Ca_{ER}}] + \frac{\rho_m}{\beta_m}[\mathrm{Ca_m}]\end{aligned} \tag{15}$$

and are then substituted into Equation 8.

B. Schnakenberg model

The Schnakenberg model is a reaction-diffusion model, which means that it is a system whose behaviour depends both on reactions between molecules and the spatial component of diffusion through the environment. The rate of change in the concentrations u and v is given by the equations

$$\begin{cases}\frac{\delta u}{\delta t} = D_u\nabla^2 u + c_1 - c_{-1}u + c_3u^2v \\ \frac{\delta v}{\delta t} = D_v\nabla^2 v + c_2 - c_3u^2v.\end{cases} \tag{16}$$

The meaning of this model on a molecular level can be deduced using the law of mass action. Firstly, the molecule U corresponding to the concentration u is added to the system by the decay of some molecule X at the rate c_1 while decaying at the rate c_{-1} into X, which is described by the reaction

$$\mathrm{X} \underset{c_{-1}}{\overset{c_1}{\rightleftharpoons}} \mathrm{U}. \tag{17}$$

Secondly, the molecule V corresponding to the concentration v is added to the system through the decay of some molecule Y at the rate c_2

$$Y \xrightarrow{c_2} \mathrm{V}. \tag{18}$$

Lastly, the factor c_3u^2v in both equations with opposite signs indicates that two molecules of U can react with a molecule of V at the rate c_3 to form an extra molecule of U, described by the reaction

$$2\mathrm{U} + \mathrm{V} \xrightarrow{c_3} 3\mathrm{U}. \tag{19}$$

There is also a spatial factor, as the molecules U and V diffuse through the system over time. Mathematically, this means that the concentration in a certain location is "pulled" towards the concentration around that location. If there were no reactions in the system, this means that the diffusion causes the concentration to spread out over the environment towards a homogeneous steady state.

The differential equations show how the concentrations in a location will affect the change in the concentrations. The rate $\frac{\delta v}{\delta t}$ decreases when u or v increases. Increasing u will either decrease or increase the rate of change $\frac{\delta u}{\delta t}$ depending on the values of c_{-1}, c_3 and the value of v in that location. For smaller concentrations of u, the rate of change in u could decrease. However, if u is large enough, the quadratic term will always eventually overpower the linear term and cause the rate of change to increase, assuming both c_3 and v are nonzero. As u increases, the quadratic term increases rapidly, which in turn decreases the rate of change in v. The quadratic term

Parameter	Value
Total concentration	
$\mathrm{Ca_{tot}}$	90 μM
$\mathrm{Pr_{tot}}$	120 μM
Geometric parameters	
ρ_{ER}	0.01
ρ_m	0.01
β_{ER}	0.0025
β_m	0.0025
Kinetics parameters	
k_{pump}	20 $\mathrm{s^{-1}}$
k_{leak}	0.05 $\mathrm{s^{-1}}$
k_{in}	300 μM $\mathrm{s^{-1}}$
k_{out}	125 $\mathrm{s^{-1}}$
k_m	0.00625 $\mathrm{s^{-1}}$
k_+	0.1 $\mu\mathrm{M^{-1}}$ $\mathrm{s^{-1}}$
k_-	0.01 $\mathrm{s^{-1}}$
K_1	5 μM
K_2	0.8 μM
K_3	5 μM

TABLE I: The fixed parameters used in the calcium oscillations model.

decreases again, and the rate of change in u can become overpowered by decay again. In this way, a homogeneous concentration is expected to show oscillating behaviour in some conditions. Because of the spatial component of this model, the system can give rise to so-called Turing patterns over time.

III. Method

THIS section will describe how the various figures for the multicompartmental model are computed. Furthermore, the methods are described for discretising the space and time in the Schnakenberg model, and the initial conditions of the environments are described.

A. Complex calcium oscillations

The calcium oscillations are studied for three different values of k_{ch}: 2830 s^{-1}, 3900 s^{-1}, and 4000 s^{-1}. The difference in k_{ch} can be caused by genetic mutations in the channels of the ER. The other parameters are set to the values displayed in Table I. Each of the three systems has initial concentrations of $[\mathrm{Ca_{cyt}}] = 0.3$, $[\mathrm{Ca_{ER}}] = 0.2$, and $[\mathrm{Ca_m}] = 1$.

Each system is numerically integrated using `scipy.integrate.odeint` [2] for $t = 0s - 1000s$. The results of this numerical integration is then plotted as a time-evolution for $t = 0s - 300s$. Furthermore, the three 2D-phase plots will be shown and possible orbits will be identified. A 3D phase plot will also be shown. These phase plots are also shown for $t = 0s - 300s$. At last, a lorentz map will be shown, which tries to find any correlation between the peaks in the calcium oscillations. These peaks are found with `scipy.signal.find_peaks` [2]. The peaks are then plotted on a scatter plot, where the x-coordinate is the value of the nth-peak and the y-coordinate is the value of the (n + 1)th-peak. This is done for $t = 100s - 1000s$, which neglects the initial settle phase.

B. Schnakenberg model

The system described in Equation 20 is solved in discrete time steps of interval length Δt using Euler's method to approximate the concentrations at a location i over time as

$$\begin{cases} u_i(t+\Delta t) = & u_i(t) \\ & +\Delta t(D_u\nabla^2 u + c_1 - c_{-1}u + c_3u^2v) \\ v_i(t+\Delta t) = & v_i(t) + \Delta t(D_v\nabla^2 v + c_2 - c_3u^2v). \end{cases} \tag{20}$$

This is done for both a 1D and 2D environment. In the 1D case, the environment is a line of length L which is discretised into N spatial points separated by intervals of length $dx = L/N$, where the location of a point is indicated by i. For any concentration z at a point i, the Laplace operator ∇^2 can be approximated by the equation

$$\nabla^2 z_i = \frac{z_{i-1} + z_{i+1} - 2z_i}{dx^2}. \tag{21}$$

The 2D case considers a square environment with sides of length L which is discretised into $N \times N$ spatial points, where the horizontal and vertical distance between the points is again $dx = L/N$. The horizontal and vertical locations are indicated by the letters i and j, respectively. Then, for a concentration z at a point (i, j), the Laplace operator can be approximated by the equation

$$\nabla^2 z_{(i,j)} = \frac{z_{i-1,j} + z_{i+1,j} + z_{i,j-1} + z_{i,j+1} - 4z_{i,j}}{dx^2} \tag{22}$$

For both environments, this report uses the parameters $c_1 = 0.1$, $c_{-1} = 1$, $c_2 = 0.9$, $c_3 = 1$, $D_u = 0.0004$, $D_v = 0.016$, $L = 1$, $N = 100$ and $\Delta t = 0.001$. The initial conditions for the 1D environment were taken to be

$$\{u_i(0), v_i(0)\} = \begin{cases} \{1, 3\} & \text{for } i = 5 \\ \{0, 0\} & \text{for } i \neq 5. \end{cases} \tag{23}$$

The initial conditions for each point in the 2D environment were taken to be random fluctuations around 1 and 3 for u and v, respectively. These random fluctuations were implemented using a random normal distribution

centered around 1 and 3 with a standard deviation of 0.01, using the function `numpy.random.normal`.

IV. Results

THE time evolution, 2D and 3D phase plots and lorentz map will be shown in this section for the multicompartmental model. The results show three distinct phases in the periodic oscillations, which can be identified in the phase plots. Additionally, the behaviour of the Schnakenberg model is shown over time and interpreted.

A. Complex calcium oscillations

The time evolution of the calcium concentrations is calculated by numerical integration of equations 8, 9, and 10. The results are plotted in Figure 1 for the case of $k_{ch} = 2830s^{-1}$, $k_{ch} = 3900s^{-1}$, and $k_{ch} = 4000s^{-1}$. All three figures show an initial setting phase before they go into periodic oscillations. The figures show that for lower values of k_{ch} the peaks of $[\mathrm{Ca_{ER}}]$ are higher, as predicted. Furthermore, the peak and dip are further apart for $k_{ch} = 2830s^{-1}$. This indicates that the ER is able to channel more calcium through its channel. Since more calcium flows through the channel into the cytosol, more calcium can be absorbed by the mitochondria. This can also be seen, since the calcium concentrations in the mitochondria is significantly higher in the case of $k_{ch} = 2830s^{-1}$ as opposed to $k_{ch} = 3900s^{-1}$ and $k_{ch} = 4000s^{-1}$.

These periodic oscillations are composed of three phases. The first phase consists of the rapid release of Ca^{2+} ions from the ER through the channels. This causes a sharp increase in calcium concentration in the cytosol and in the mitochondria.

The second phase consists of the slow release of Ca from the mitochondria. This slow release allows for the binding of calcium with the proteins to form CaPr. Meanwhile, the ER and cytosol exchange calcium at a much faster rate, causing the small oscillations within the periodic oscillations.

The third phase starts when the mitochondria reach their equilibrium state. Therefore, there are effectively no free calcium ions released into the cytosol and the decay of CaPr becomes the major reaction. The decay results in calcium atoms, which are pumped into the ER. Thus the concentration of calcium increases in the ER, until the calcium ions are released again through the channels, which brings the system back to phase one.

The time-evolution of the systems is also captured in three 2D phase plots. Figures 2, 3, and 4 show the three 2D-phase plots for $k_{ch} = 2830s^{-1}$, $k_{ch} = 3900s^{-1}$, and $k_{ch} = 4000s^{-1}$ respectively.

The phase plots of $[\mathrm{Ca_{ER}}]$ and $[\mathrm{Ca_{cyt}}]$ show a stable limit cycle for the calcium concentrations in ER and cytosol for all three values of k_{ch}. The large cycle corresponds with phases 1 and 3, while the small cycle within the large cycle corresponds with the oscillations of phase 2.

The phase plots of $[\mathrm{Ca_m}]$ and $[\mathrm{Ca_{ER}}]$ show three limit cycles for the cases of $k_{ch} = 3900s^{-1}$ and $k_{ch} = 4000s^{-1}$. The upper and lower "triangle" are unstable limit cycles, and are obtained due to the initial setting phase. The system with $k_{ch} = 2830s^{-1}$ is able to able to reach its periodic state much faster, therefore, those two "triangles" can not be seen in its phase plot. The main "triangle" is a stable limit cycle. The diagonal line in the limit cycle is created due to phase 1, where calcium ions are ejected from the ER and captured in the mitochondria. The vertical line is then created through phase 2, where the mitochondria release their calcium and the ER undergoes its oscillations. Finally, the horizontal line is created due to phase 3, where the calcium atoms are pumped into the ER after they are released from the CaPr decay.

The phase plots of $[\mathrm{Ca_{cyt}}]$ and $[\mathrm{Ca_m}]$ in the case of $k_{ch} = 3900s^{-1}$ and $k_{ch} = 4000s^{-1}$ again show three limit cycles, with the left and right cycle being unstable. This is again due to the initial setting phase. The system with $k_{ch} = 2830s^{-1}$ misses this initial phase and therefore only has one limit cycle. The main cycle is stable. Phase 1 results in the vertical line from the bottom to the top, which then goes to the right where it reaches the oscillation part. In phase 2 the concentration in the mitochondria reduces, which makes the phase plot go to the left. Before it reached phase 3, where it goes down again to the bottom.

Figures 5, 6, and 7 show the 3D phase plot of the three systems. The three phases can be retrieved from all three systems. Phase 1 can be seen at the location where $\mathrm{Ca_{cyt}}$ is low, but $\mathrm{Ca_{ER}}$ is high. Phase 2 can be easily identified by the oscillating behaviour. Phase 3 then occurs after the oscillations and goes back to low values of $\mathrm{Ca_{cyt}}$ and high values of $\mathrm{Ca_{ER}}$.

At last, the lorentz map for all three systems is shown in figures 8, 9, and 10 for the calcium concentrations of the mitochondria for the cases $k_{ch} = 2830s^{-1}$, $k_{ch} = 3900s^{-1}$, and $k_{ch} = 4000s^{-1}$ respectively. The lorentz map shows whether it is possible to predict the value of the next peak based on the current peak.

Figure 8, $k_{ch} = 2830s^{-1}$, shows a lorentz map, where a curve seems to be forming, which would indicate that the peaks are deterministic. They can be predicted once

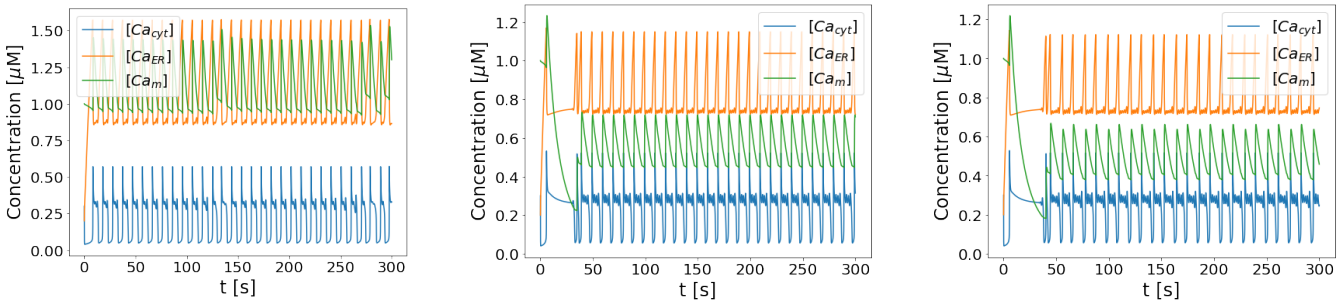

(a) $k_{ch} = 2830s^{-1}$ (b) $k_{ch} = 3900^{-1}$ (c) $k_{ch} = 4000^{-1}$

Fig. 1: The time evolution of the calcium concentrations with initial conditions $[\mathrm{Ca_{cyt}}] = 0.3$, $[\mathrm{Ca_{ER}}] = 0.2$, and $[\mathrm{Ca_m}] = 1$. This is performed for three values of k_{ch}. The other parameters of the system are given in Table I.

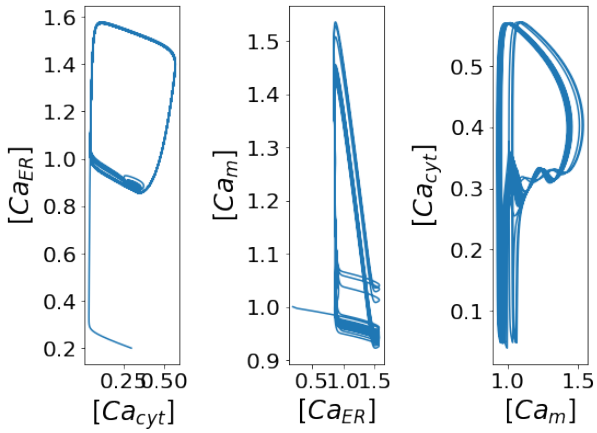

Fig. 2: The three phase plots of the calcium concentrations. The system had initial conditions $[\mathrm{Ca_{cyt}}] = 0.3$, $[\mathrm{Ca_{ER}}] = 0.2$, and $[\mathrm{Ca_m}] = 1$, and $k_{ch} = 2830s^{-1}$. The other parameters are given in Table I. The system ran until $t = 300s$. The left plot shows the phase plot for the concentrations of $\mathrm{Ca_{ER}}$ and $\mathrm{Ca_{cyt}}$. The middle plot shows the phase plot for the concentrations of $\mathrm{Ca_m}$ and $\mathrm{Ca_{ER}}$. The right plot shows the phase plot for the concentrations of $\mathrm{Ca_{cyt}}$ and $\mathrm{Ca_m}$.

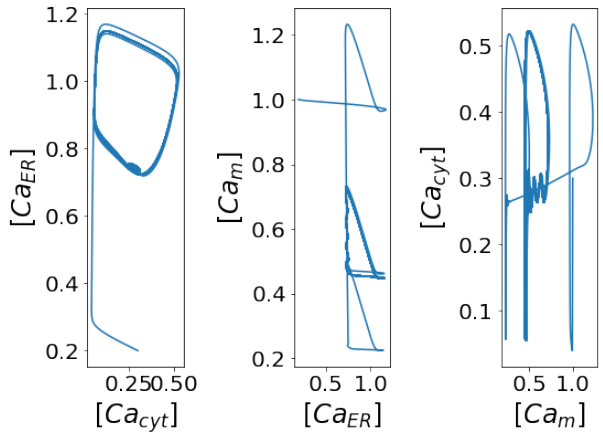

Fig. 3: The three phase plots of the calcium concentrations. The system had initial conditions $[\mathrm{Ca_{cyt}}] = 0.3$, $[\mathrm{Ca_{ER}}] = 0.2$, and $[\mathrm{Ca_m}] = 1$, and $k_{ch} = 3900s^{-1}$. The other parameters are given in Table I. The system ran until $t = 300s$. The left plot shows the phase plot for the concentrations of $\mathrm{Ca_{ER}}$ and $\mathrm{Ca_{cyt}}$. The middle plot shows the phase plot for the concentrations of $\mathrm{Ca_m}$ and $\mathrm{Ca_{ER}}$. The right plot shows the phase plot for the concentrations of $\mathrm{Ca_{cyt}}$ and $\mathrm{Ca_m}$.

the curve is known. This curve could be obtained by running the system for longer. The curve would then be populated by more peaks, until a solid curve appears.

Figure 9, $k_{ch} = 3900s^{-1}$, shows that the peak values are all within a very small range. The range is in the order of 10^{-7}. You can make a very precise guess on the next peak value given the current peak value.

Figure 10, $k_{ch} = 4000s^{-1}$, shows a completely different result. The system only has two peak values at 0.637 and 0.662 μM. These peaks follow each other up. If a peak value of 0.662 occurs then the next peak value will be at 0.637 and vice versa.

B. Schnakenberg model

Figure 11 shows the development of the concentrations u and v over time by indicating the concentrations by colors at different time points on the vertical axis.

The concentrations are initially zero everywhere except for the one point at $i = 5$. Because u and v are (close to) zero throughout most of the environment, the initial period is dominated by diffusion and the addition terms c_1 and c_2 in the differential equations, causing the concentrations to steadily increase initially. The higher concentration "sources" from the initial condition spread through the environment, and because they originated from such a small point, they do not significantly impact

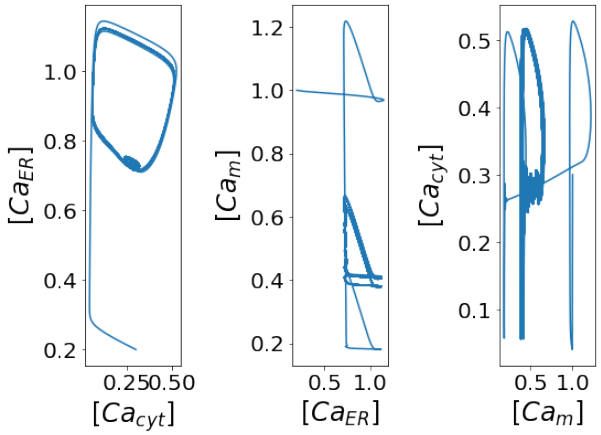

Fig. 4: The three phase plots of the calcium concentrations. The system had initial conditions $[\mathrm{Ca_{cyt}}] = 0.3$, $[\mathrm{Ca_{ER}}] = 0.2$, and $[\mathrm{Ca_m}] = 1$, and $k_{ch} = 4000s^{-1}$. The other parameters are given in Table I. The system ran until $t = 300s$. The left plot shows the phase plot for the concentrations of $\mathrm{Ca_{ER}}$ and $\mathrm{Ca_{cyt}}$. The middle plot shows the phase plot for the concentrations of $\mathrm{Ca_m}$ and $\mathrm{Ca_{ER}}$. The right plot shows the phase plot for the concentrations of $\mathrm{Ca_{cyt}}$ and $\mathrm{Ca_m}$.

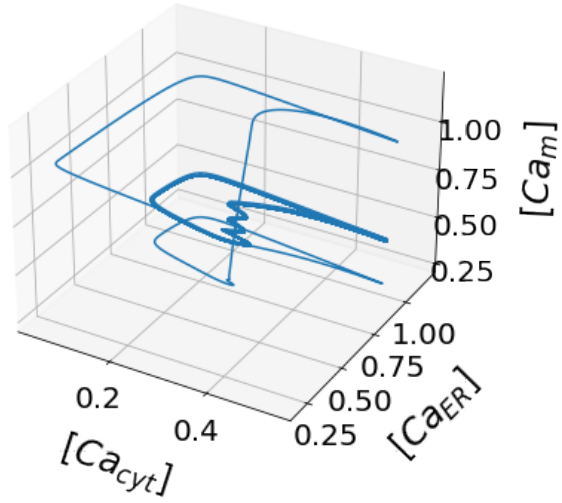

Fig. 6: A 3D phase plot for the calcium concentrations in the system. The system had initial conditions $[\mathrm{Ca_{cyt}}] = 0.3$, $[\mathrm{Ca_{ER}}] = 0.2$, and $[\mathrm{Ca_m}] = 1$, and $k_{ch} = 3900s^{-1}$. The other parameters are given in Table I. The system ran until $t = 300s$.

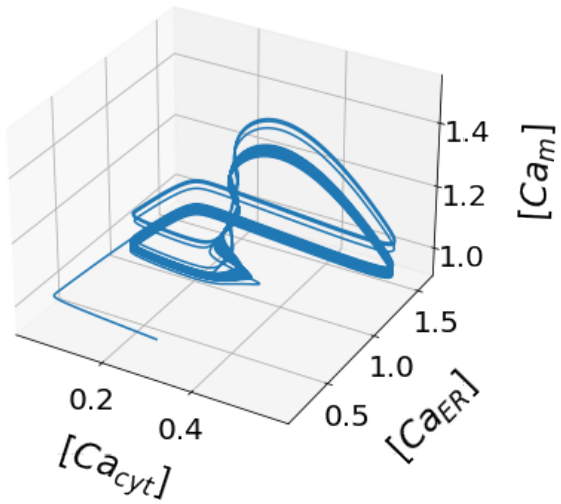

Fig. 5: A 3D phase plot for the calcium concentrations in the system. The system had initial conditions $[\mathrm{Ca_{cyt}}] = 0.3$, $[\mathrm{Ca_{ER}}] = 0.2$, and $[\mathrm{Ca_m}] = 1$, and $k_{ch} = 28303s^{-1}$. The other parameters are given in Table I. The system ran until $t = 300s$.

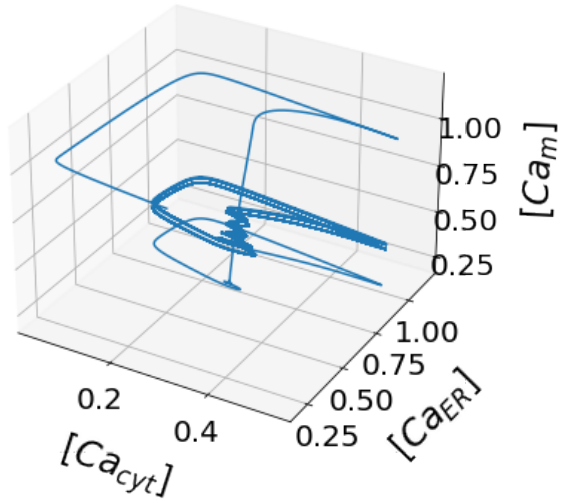

Fig. 7: A 3D phase plot for the calcium concentrations in the system. The system had initial conditions $[\mathrm{Ca_{cyt}}] = 0.3$, $[\mathrm{Ca_{ER}}] = 0.2$, and $[\mathrm{Ca_m}] = 1$, and $k_{ch} = 4000s^{-1}$. The other parameters are given in Table I. The system ran until $t = 300s$.

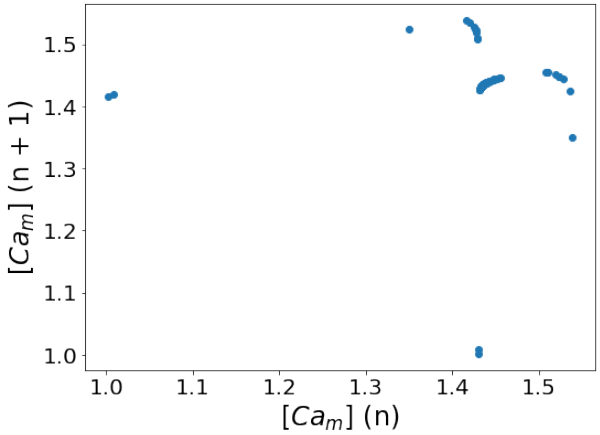

Fig. 8: The lorentz map of the peaks of the $\mathrm{Ca_m}$ concentration. The system had initial conditions $[\mathrm{Ca_{cyt}}] = 0.3$, $[\mathrm{Ca_{ER}}] = 0.2$, and $[\mathrm{Ca_m}] = 1$, and $k_{ch} = 2830s^{-1}$. The other parameters are given in Table I. The peaks are obtained from $t = 100s$ to $t = 1000s$. The peaks seem to be forming a curve, which indicates that the peaks are deterministic.

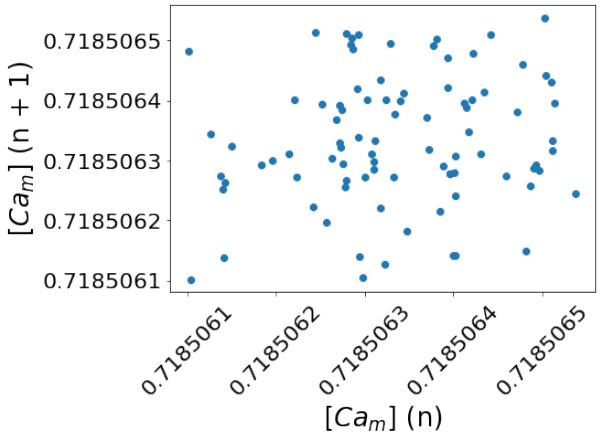

Fig. 9: The lorentz map of the peaks of the $\mathrm{Ca_m}$ concentration. The system had initial conditions $[\mathrm{Ca_{cyt}}] = 0.3$, $[\mathrm{Ca_{ER}}] = 0.2$, and $[\mathrm{Ca_m}] = 1$, and $k_{ch} = 3900s^{-1}$. The other parameters are given in Table I. The peaks are obtained from $t = 100s$ to $t = 1000s$. All peak values have about the same peak value. The range of peak values is in the order of 10^{-7}.

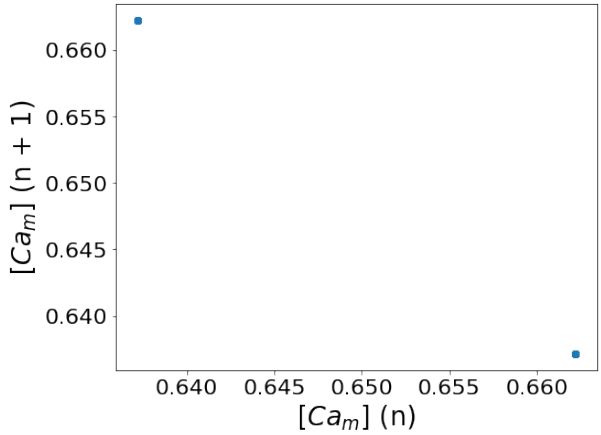

Fig. 10: The lorentz map of the peaks of the $\mathrm{Ca_m}$ concentration. The system had initial conditions $[\mathrm{Ca_{cyt}}] = 0.3$, $[\mathrm{Ca_{ER}}] = 0.2$, and $[\mathrm{Ca_m}] = 1$, and $k_{ch} = 4000s^{-1}$. The other parameters are given in Table I. The peaks are obtained from $t = 100s$ to $t = 1000s$. There are only two peak values present. These peak values follow each other up and are thus easily predicted given the current peak value.

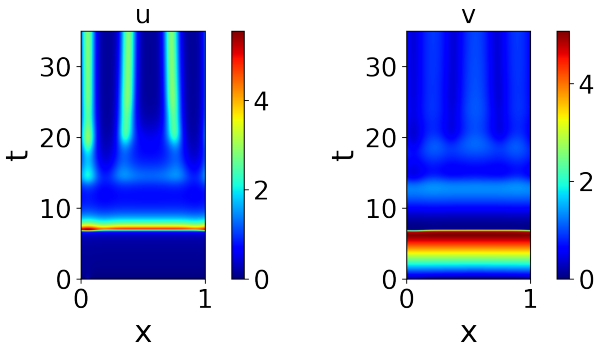

(a) (b)

Fig. 11: The development of the concentrations u and v in the 1D Schnakenberg model over time, using the parameters $c_1 = 0.1$, $c_{-1} = 1$, $c_2 = 0.9$, $c_3 = 1$, $D_u = 0.0004$, $D_v = 0.016$, $L = 1$, $N = 100$ and $\Delta t = 0.001$.

the overall environment yet. Because $c_{-1} = 0.9$ and c_1 is only 0.1, U decays quite more quickly than it forms, causing its concentration not to rise significantly. v does keep rising steadily, since v has no decay term. Once the concentrations are high enough, the term c_3u^2v starts to overpower the other terms, increasing the rate of change of u. As u increases, that term starts increasing even more quickly because it depends on the square of u. This causes u to rapidly increase. However the rate of change of v subtracts that same term, so as u rises, v quickly starts to decrease. The term c_3u^2v becomes very small again, and the rate of change in u is mostly dominated by decay again, causing its concentration to decrease again.

Because of the initial conditions, the concentration fields are not homogeneous and differ slightly. This means the system does not move to a homogeneous steady state, since that state is unstable against spatial variation. Because v diffuses more quickly than u, it can slow down the production of u over a larger area. This causes areas with higher concentrations of u to stay high as the concentration can not spread as far and they

consume v. The pattern of three high-concentration areas forms as a result.

Figure 12 shows the concentrations u and v at six different time points for the 2D Schnakenberg model. In the first period before the patterns form, the concentrations increase and decrease in quick succession. First, v quickly decreases because of the negative term in its differential equation, while u increases because of that same positive term. Once u and v are very low, the c_2 term dominates the rate of change in v again and v steadily starts rising. After a while, the c_3u^2v is large enough again for u to increase and v to decrease, and this process repeats. At this stage, the noise that was present in the initial conditions is not yet strong enough to show significant effects. However at a certain point, the irregularities in the concentrations start to become apparent. Similar to the 1D case, several high-concentration areas start to form in u. These areas have a repellent effect on each other, and they start to "move" and spread out in such a way that they each have a roughly similar distance from each other. Furthermore, these areas develop to each have a very similar size and concentration. This repetitive pattern is a Turing pattern, as expected.

V. Discussion & Conclusion

THE report was able to implement two different spatial models: a multicompartmental model and a grid based model.

The multicompartmental model was implemented on a cell to study the dynamics of calcium concentrations in the ER, mitochondria and cytosol. The report found that genetic mutations in the ER channels also has effects on the other compartments. A lower value for k_{ch} increased the peaks and dips of the calcium concentration in the ER and increased the concentration levels in the mitochondria. The lowest value of k_{ch} also removed the initial settle phase. This removed two of the unstable limit cycles, which were present for $k_{ch} = 3900s^{-1}$ and $k_{ch} = 4000s^{-1}$.

Furthermore, the three different values of k_{ch} showed a difference peak dynamics as shown in the lorentz maps. $k_{ch} = 2830s^{-1}$ showed that the peak values follow a curve and are not deterministic. The system needs to run for longer to obtain the entire curve and could be of interest to do follow up research on.

$k_{ch} = 3900s^{-1}$ showed that all peak values have approximately the same value. The case of $k_{ch} = 4000s^{-1}$ showed two possible peaks at 0.637 and 0.662 μM. These peaks follow each other up.

The Schnakenberg model was implemented and showed the forming of Turing patterns over time in both the 1D and 2D environment. Future research could investigate how these patterns depend on the chosen parameters and initial conditions. It is unclear whether these Turing patterns emerge for all inhomogeneous initial conditions, or whether they require a specific range of configurations.

References

[1] M. Marhl, T. Haberichter, M. Brumen, and R. Heinrich, "Complex calcium oscillations and the role of mitochondria and cytosolic proteins," *Biosystems*, vol. 57, no. 2, pp. 75–86, 2000.

[2] P. Virtanen, R. Gommers, T. E. Oliphant, M. Haberland, T. Reddy, D. Cournapeau, E. Burovski, P. Peterson, W. Weckesser, J. Bright, S. J. van der Walt, M. Brett, J. Wilson, K. J. Millman, N. Mayorov, A. R. J. Nelson, E. Jones, R. Kern, E. Larson, C. J. Carey, İ. Polat, Y. Feng, E. W. Moore, J. VanderPlas, D. Laxalde, J. Perktold, R. Cimrman, I. Henriksen, E. A. Quintero, C. R. Harris, A. M. Archibald, A. H. Ribeiro, F. Pedregosa, P. van Mulbregt, and SciPy 1.0 Contributors, "SciPy 1.0: Fundamental Algorithms for Scientific Computing in Python," *Nature Methods*, vol. 17, pp. 261–272, 2020.

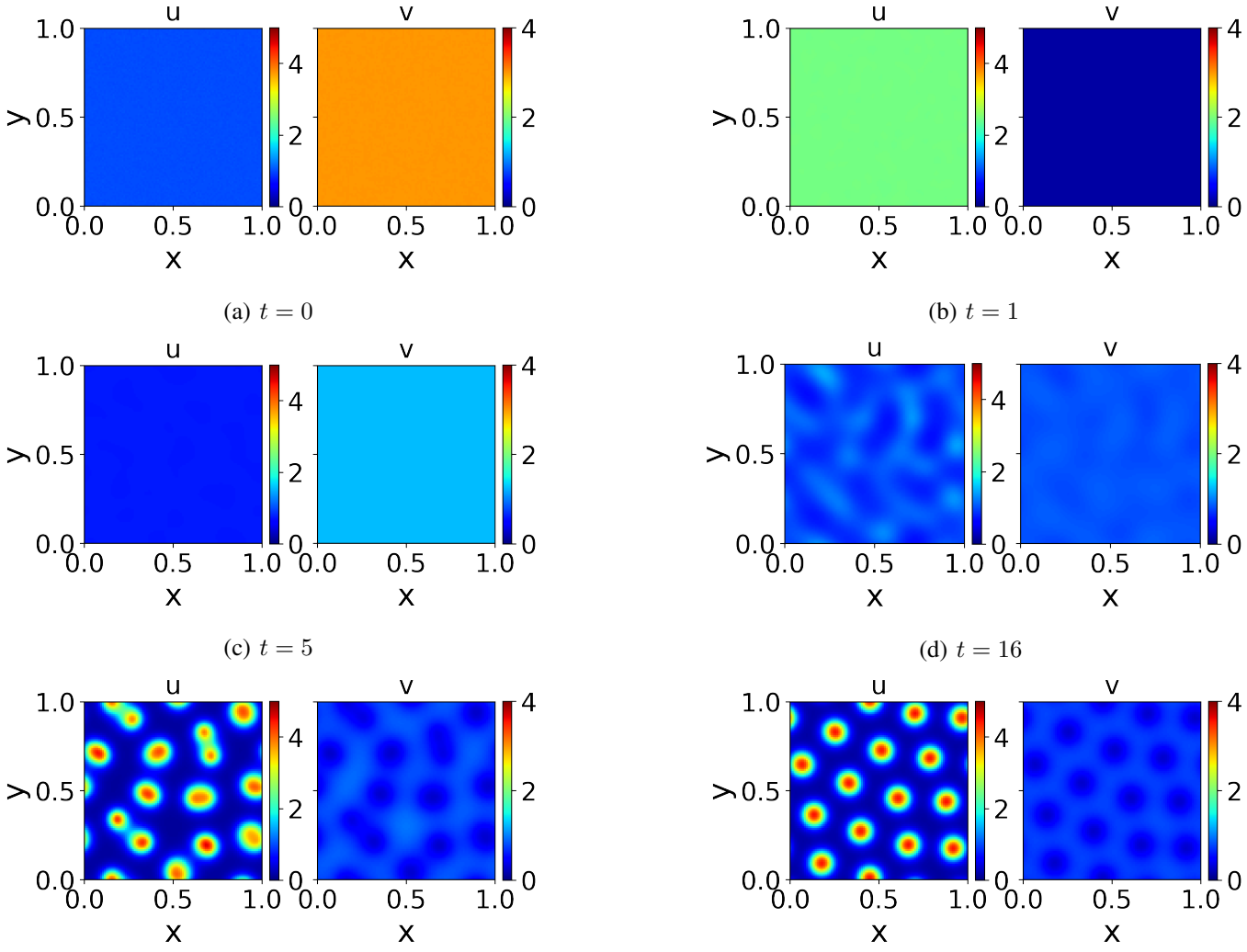

(a) $t = 0$

(b) $t = 1$

(c) $t = 5$

(d) $t = 16$

(e) $t = 30$

(f) $t = 300$

Fig. 12: The concentrations u and v in the 2D Schnakenberg model at different time points, using the parameters $c_1 = 0.1$, $c_{-1} = 1$, $c_2 = 0.9$, $c_3 = 1$, $D_u = 0.0004$, $D_v = 0.016$, $L = 1$, $N = 100$ and $\Delta t = 0.001$.